

4

AD-A190 812

DTIC FILL COPY

CHARACTERIZATION AND MODELING OF THORACO-ABDOMINAL RESPONSE TO BLAST WAVES

Volume 7. Gastrointestinal Response to Blast

Annual/Final Report

*Original contains color
plates: All DTIC reproductions
will be in black and
white*

May 1985

DTIC
ELECTE
FEB 16 1988
S D

Cheng J. Chuong
James H.-Y. Yu
Edward J. Vasel
James H. Stuhmiller, Principal Investigator

JAYCOR
11011 Torreyana Road
San Diego, California 92121

Contract No. DAMD17-82-C-2062

Supported by

U. S. Army Medical Research and Development Command
Fort Detrick, Frederick, Maryland 21701

The findings in this report are not to be construed as an official Department of the Army position unless so designated by other authorized documents.

Accession For	
NTIS CRA&I	<input checked="" type="checkbox"/>
DTIC TAB	<input type="checkbox"/>
Unannounced	<input type="checkbox"/>
Justification	
By	
Distribution/	
Availability Codes	
Dist	Avail and/or Special
A-1	

UNCLASSIFIED
2

REPORT DOCUMENTATION PAGE

Form Approved
OMB No. 0704-0188

1a. REPORT SECURITY CLASSIFICATION UNCLASSIFIED		1b. RESTRICTIVE MARKINGS	
2a. SECURITY CLASSIFICATION AUTHORITY		3. DISTRIBUTION/AVAILABILITY OF REPORT Approved for public release; distribution unlimited	
2b. DECLASSIFICATION/DOWNGRADING SCHEDULE		4. PERFORMING ORGANIZATION REPORT NUMBER(S)	
4. PERFORMING ORGANIZATION REPORT NUMBER(S)		5. MONITORING ORGANIZATION REPORT NUMBER(S)	
6a. NAME OF PERFORMING ORGANIZATION JAYCOR	6b. OFFICE SYMBOL (If applicable)	7a. NAME OF MONITORING ORGANIZATION	
6c. ADDRESS (City, State, and ZIP Code) 11011 Torreyana Road San Diego, California 92121		7b. ADDRESS (City, State, and ZIP Code)	
8a. NAME OF FUNDING/SPONSORING ORGANIZATION U.S. Army Medical Research & Development Command	8b. OFFICE SYMBOL (If applicable)	9. PROCUREMENT INSTRUMENT IDENTIFICATION NUMBER DAMD17-82-C-2062	
8c. ADDRESS (City, State, and ZIP Code) Fort Detrick Frederick, Maryland 21701-5012		10. SOURCE OF FUNDING NUMBERS	
		PROGRAM ELEMENT NO. 61102A	PROJECT NO. 3M1 61102BS10
		TASK NO. CG	WORK UNIT ACCESSION NO. 087
11. TITLE (Include Security Classification) (U) Characterization and Modeling of Thoraco-Abdominal Response to Blast Waves Volume 7. Gastrointestinal Response to Blast			
12. PERSONAL AUTHOR(S) Cheng J. Chuong, James H.-Y. Lu, Edward Vassel, and James H. Strihmiller			
13a. TYPE OF REPORT Annual/Final	13b. TIME COVERED FROM 2/15/82 TO 5/31/85	14. DATE OF REPORT (Year, Month, Day) 1985 May	15. PAGE COUNT 38
16. SUPPLEMENTARY NOTATION Annual covers time period of 15 February 1984 - 31 May 1985. Annual/Final published in 8 volumes			
17. COORDINATE CODES		18. SUBJECT TERMS (Continue on reverse if necessary and identify by block number)	
FIELD	GROUP	SUB-GROUP	
06	21		
06	17		
19. ABSTRACT (Continue on reverse if necessary and identify by block number)			
20. DISTRIBUTION/AVAILABILITY OF ABSTRACT <input type="checkbox"/> UNCLASSIFIED/UNLIMITED <input checked="" type="checkbox"/> SAME AS RPT. <input type="checkbox"/> DTIC USERS		21. ABSTRACT SECURITY CLASSIFICATION Unclassified	
22a. NAME OF RESPONSIBLE INDIVIDUAL Mary Frances Bostian		22b. TELEPHONE (Include Area Code) 301-663-7325	22c. OFFICE SYMBOL SCRD-RMI-S

FOREWORD

This Annual/Final Report has eight volumes. The titles are as follows:

1. Project Summary
2. Blast Load Definition on a Torso Model
3. Lung Dynamics and Mechanical Properties Determination
4. Biomechanical Model of Thorax Response to Blast Loading
5. Experimental Investigation of Lung Injury Mechanism
6. Biomechanical Model of Lung Injury Mechanisms
7. Gastrointestinal Response to Blast
8. Effect of Clothing on Thoracic Response

CONTENTS

	<u>Page</u>
1. INTRODUCTION	1
2. A SIMPLIFIED FINITE ELEMENT ANALYSIS	3
3. LABORATORY TESTS OF BLAST EFFECTS ON SIMULATED GASTROINTESTINAL EMBOLI	21
Experimental Setup	21
Test Results and Discussion	25

ILLUSTRATIONS

	<u>Page</u>
2-1. Finite element model of one octant of idealized GI tract	5
2-2. Displacement time history for top surface when tube is filled with water and the bubble is at the top (Young's modulus is 1500 psi)	6
2-3. Displacement time history for top surface when tube is filled with "gel" and the bubble is at the top (Young's modulus is 1500 psi)	9
2-4. Displacement time history for top surface when tube is filled with water and bubble is at the center of the tube (Young's modulus is 1500 psi)	12
2-5. Displacement time history for top surface when tube is filled with water and bubble is at the center (Young's modulus is 3000 psi)	15
2-6. Displacement time history for top surface when tube is filled with water and bubble is at top (Young's modulus is 3000 psi)	18
3-1. Schematic of jet impactor test setup	22
3-2. Experimental setup	23
3-3. Valve and orifice plate assembly	23
3-4. Cut-away view of pressure chamber setup for simulated GI tract bubble experiment	24
3-5. Initial test installation with 0.5" air bubble	26
3-6. Transducer location on test chamber wall	26
3-7. Initial peak	27
3-8. Typical full impulse shape	27
3-9. Correlation of bubble motion with pressure	29
3-10. Intestine model	31
3-11. Intestine model installation	31

TABLE

	<u>Page</u>
3-1. Test matrix	28

1. INTRODUCTION

Injury to the wall of the large intestine has emerged as having a lower threshold for occurrence than lung injury in the qualitative animal tests made to date. The presence of gas in the form of bubbles is certainly the source of the organ's compliancy, but the exact cause and effect relation to injury is only speculative at this time. At the first quarter's review meeting, there was considerable discussion on this point and on the relevance and interpretation of bubble-in-gel experiments proposed for the BOP program. Consequently, it was decided to conduct an analysis of the intestine to guide future experimental work and to conduct preliminary blast exposure tests. Further investigation of these issues can be found in the final report "Experimental Study of the Correlation between Gastro-Intestinal Injury and Blast Loading."

2. A SIMPLIFIED FINITE ELEMENT ANALYSIS

Water is an incompressible liquid that supports only viscous stress (due to shear velocity); gel is an incompressible solid that supports only elastic stress (due to shear displacement); intestinal contents are a gas-liquid-solid slurry that probably has visco-elastic properties. One important aspect of any physical simulation to idealize the injury mechanism is the choice of material properties of the contents.

To help answer this question we have conducted an analytical study of the dynamics of an air-containing tube. For convenience, the geometry of the tube section is a rectangle (1.0" x 1.4" x 1.0") and the material composite is: an elastic outer skin, thickness 0.05" and variable elasticity; a rectangular air cavity that can be anywhere within the tube; and a filling material that is either an elastic solid (gel), an incompressible liquid (water), or a combination. By symmetry, only one octant needs to be considered in the calculation and a perspective drawing of that sector is shown in Figure 2-1. For convenience in visualizing the fluid surface displacements, however, the symmetry operators have been used to reconstruct the entire surface.

The simulations presented here consider the difference in response between liquid and elastic solid; bubble near the surface and on the centerline; and variations in the elasticity of the skin material. The results are completely qualitative at this stage because the material property constants used in the calculations do not necessarily correspond to water, gel, and intestinal wall. Rather, they are extremes that show the trends that could be expected and suggest further analyses. Furthermore, these initial calculations did not surround the casing with water; the lack of that added inertia will affect the amplitude and frequency of the response. All of these differences can be eliminated in the future.

A pressure field similar to that seen in the experiments described in Section 7 (rise time: 1.2 msec, peak pressure: 40 psi, tail pressure: 15 psi) was applied everywhere on the outer surface. Figure 2-2 shows the surface displacement time history when the bubble is at the surface and the tube is

filled with water. The Young's modulus for the skin is 1500 psi. Waves along the water-skin interface can be seen. Figure 2-3 shows the same situation when the tube is filled with gel. The stress is now absorbed by the elasticity of the gel and the surface displacement occurs only at the bubble site, where the edge stress is large. Figure 2-4 shows the displacement when the bubble is at the center of the water-filled tube. The displacement is less but similar to the earlier case. For the elastic solid case when the bubble is in the center no displacement can be seen.

The shear modulus for the elastic solid may be too great to represent gel, but the results above show that the qualitative behavior of a physical simulation could differ considerably between water and gel.

An additional calculation was made to explore the effects of wall tension. Figures 2-5 and 2-6 shows the response when the Young's modulus is set to 3000 psi. The difference in stiffness has the expected effects on amplitude and frequency of the response.

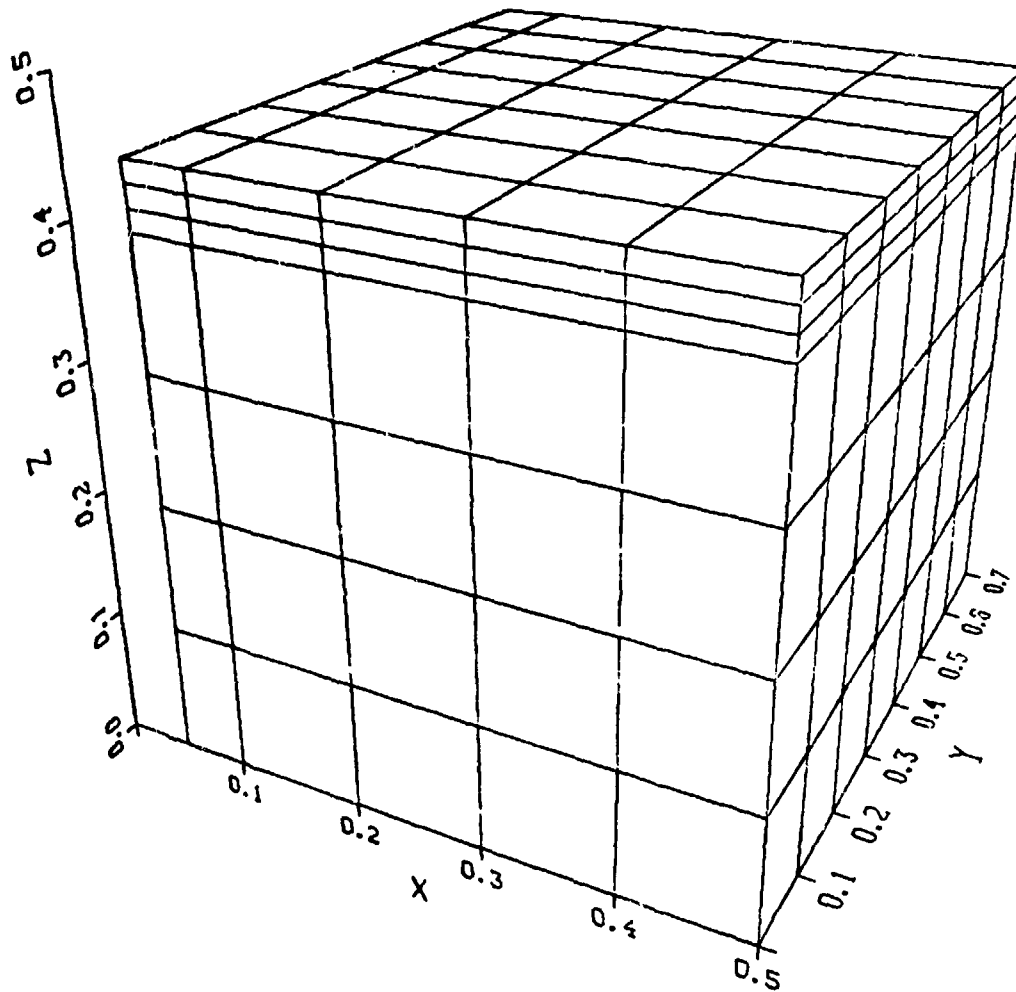


Figure 2-1. Finite element model of one octant of idealized GI tract.

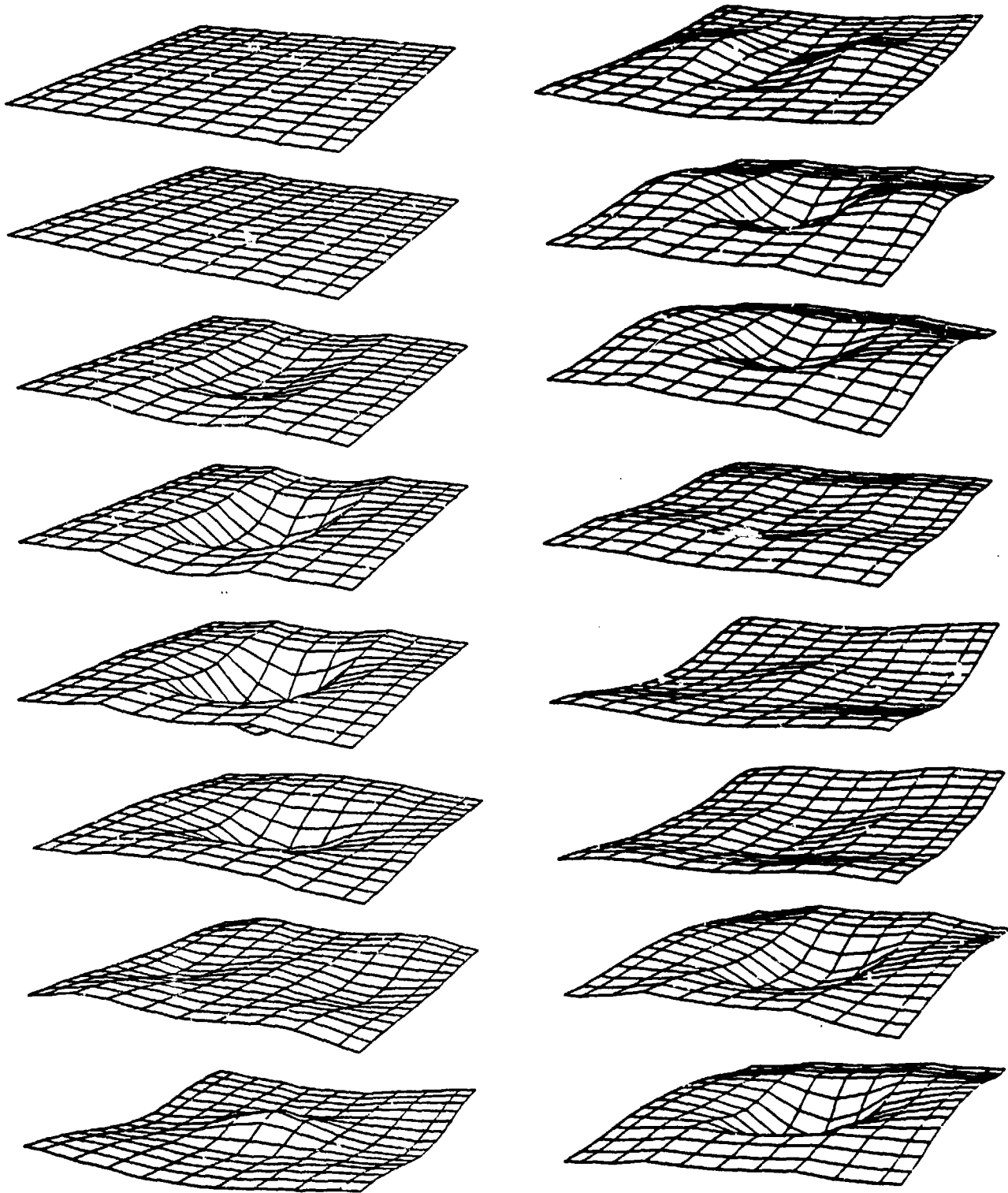


Figure 2-2. Displacement time history for top surface when tube is filled with water and the bubble is at the top. Young's modulus of the skin is 1500 psi. Each picture is at 0.4 msec intervals in all subsequent figures.

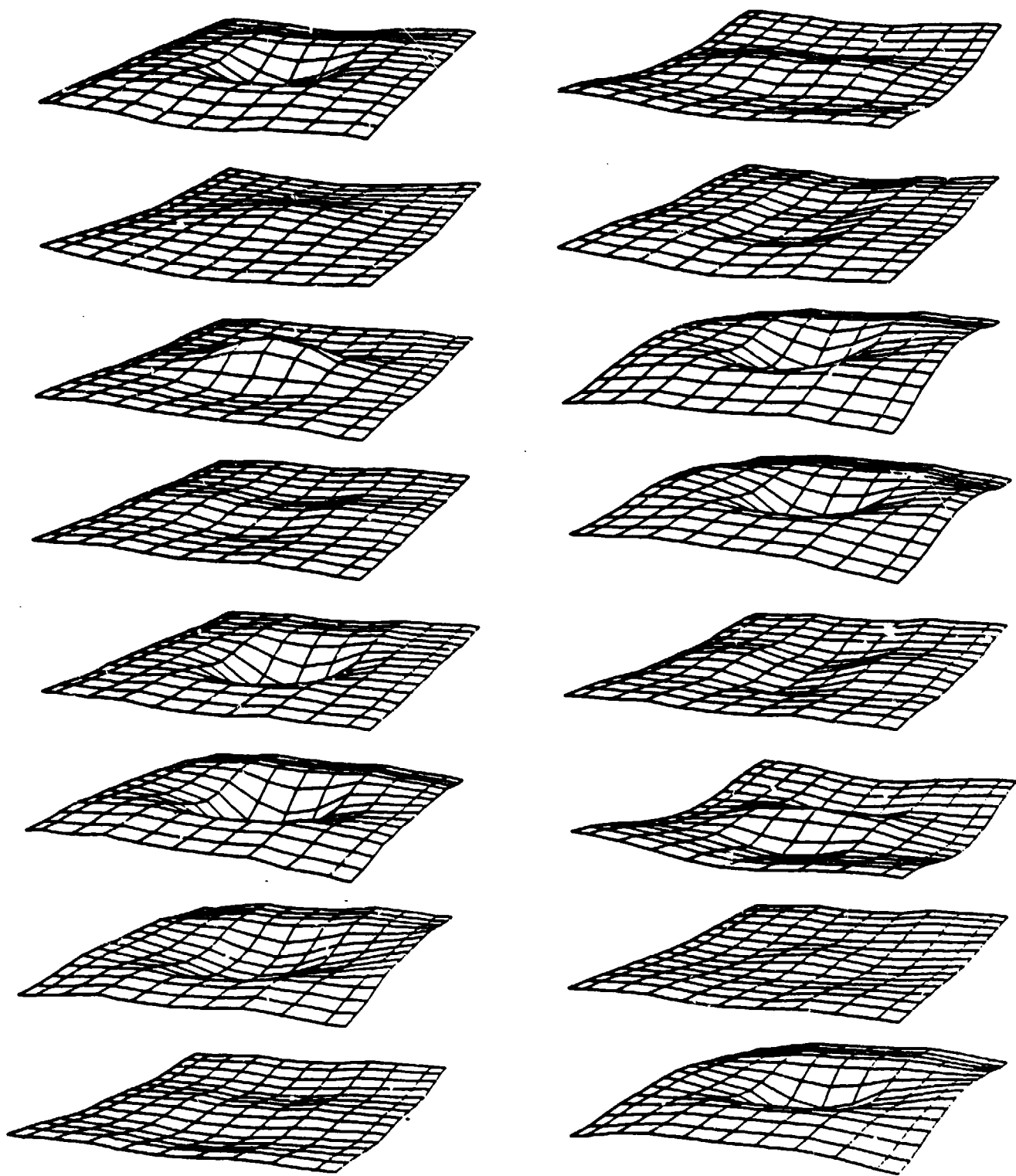


Figure 2-2. (Cont'd).

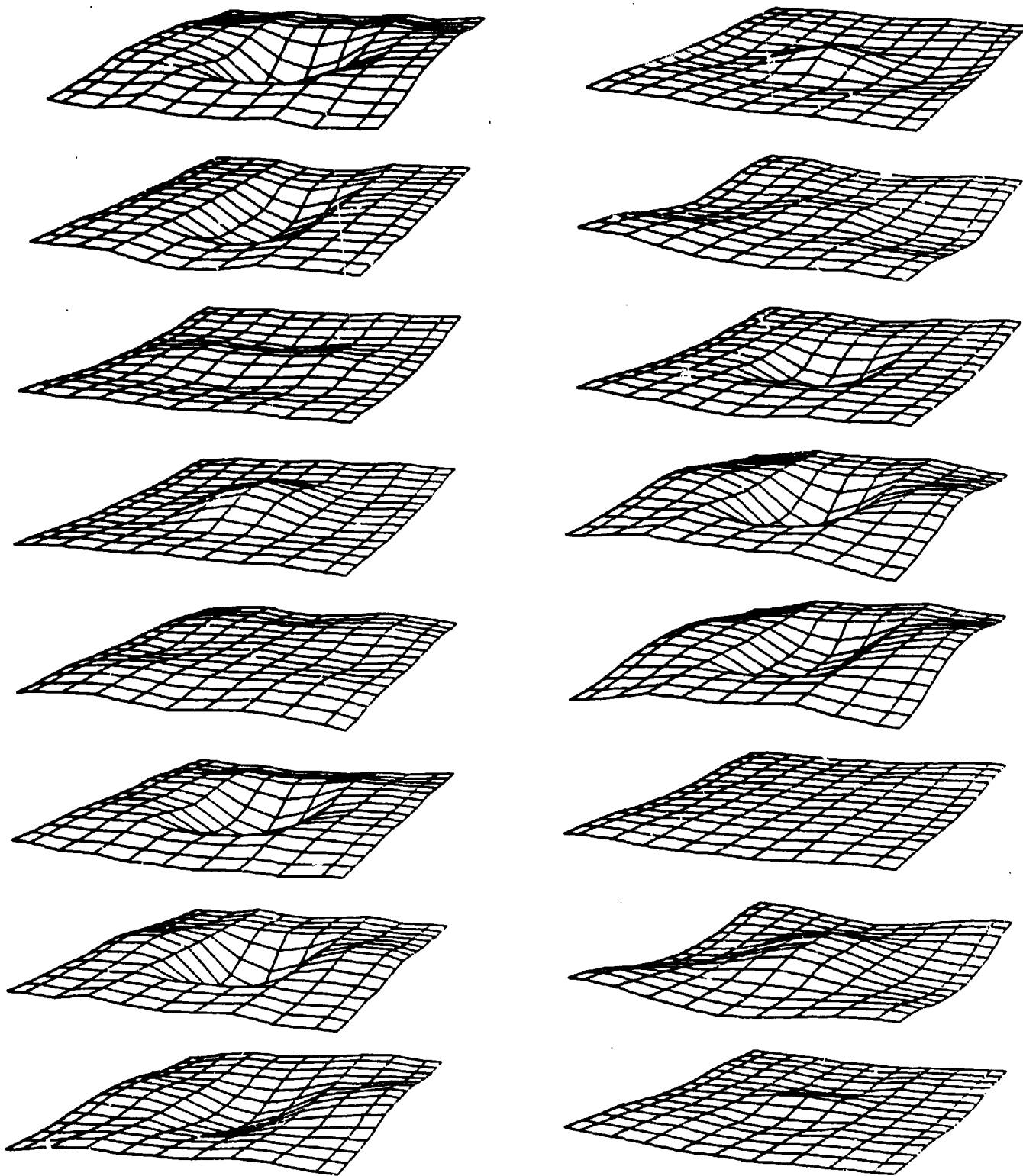


Figure 2-2. (Cont'd).

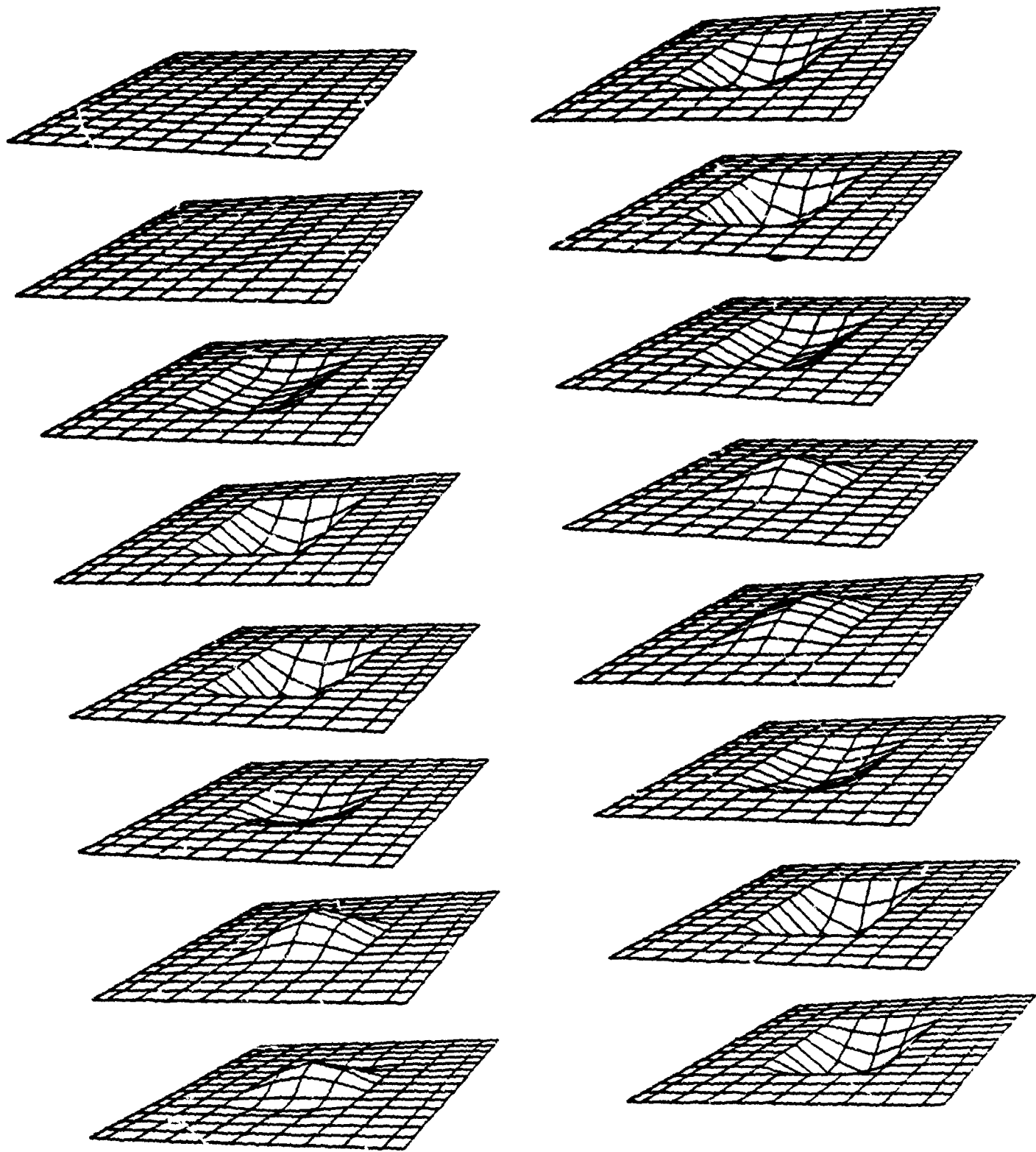


Figure 2-3. Displacement time history for top surface when tube is filled with "gel" and the bubble is at the top. Young's modulus for the skin is 1500 psi.

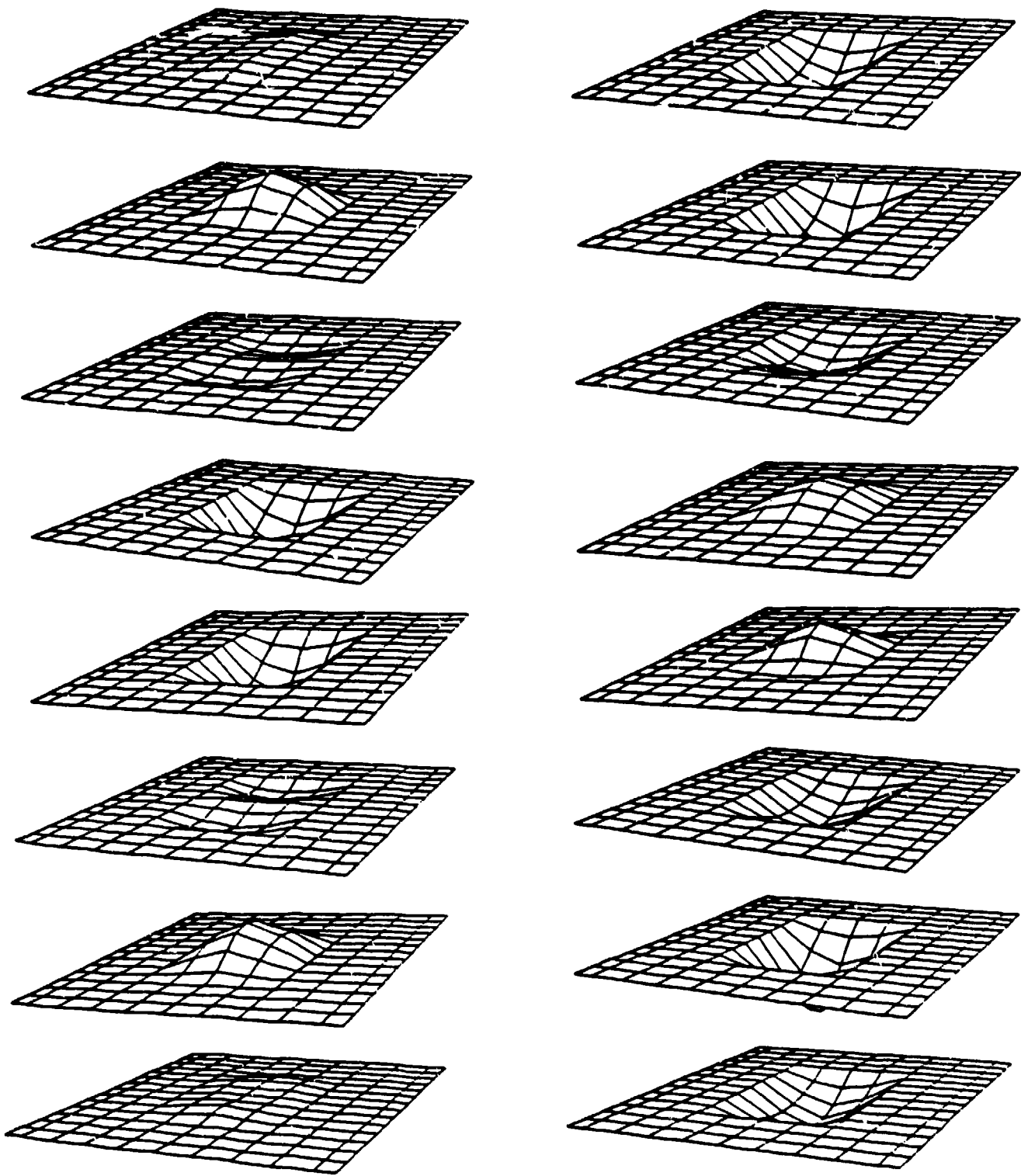


Figure 2-3. (Cont'd).

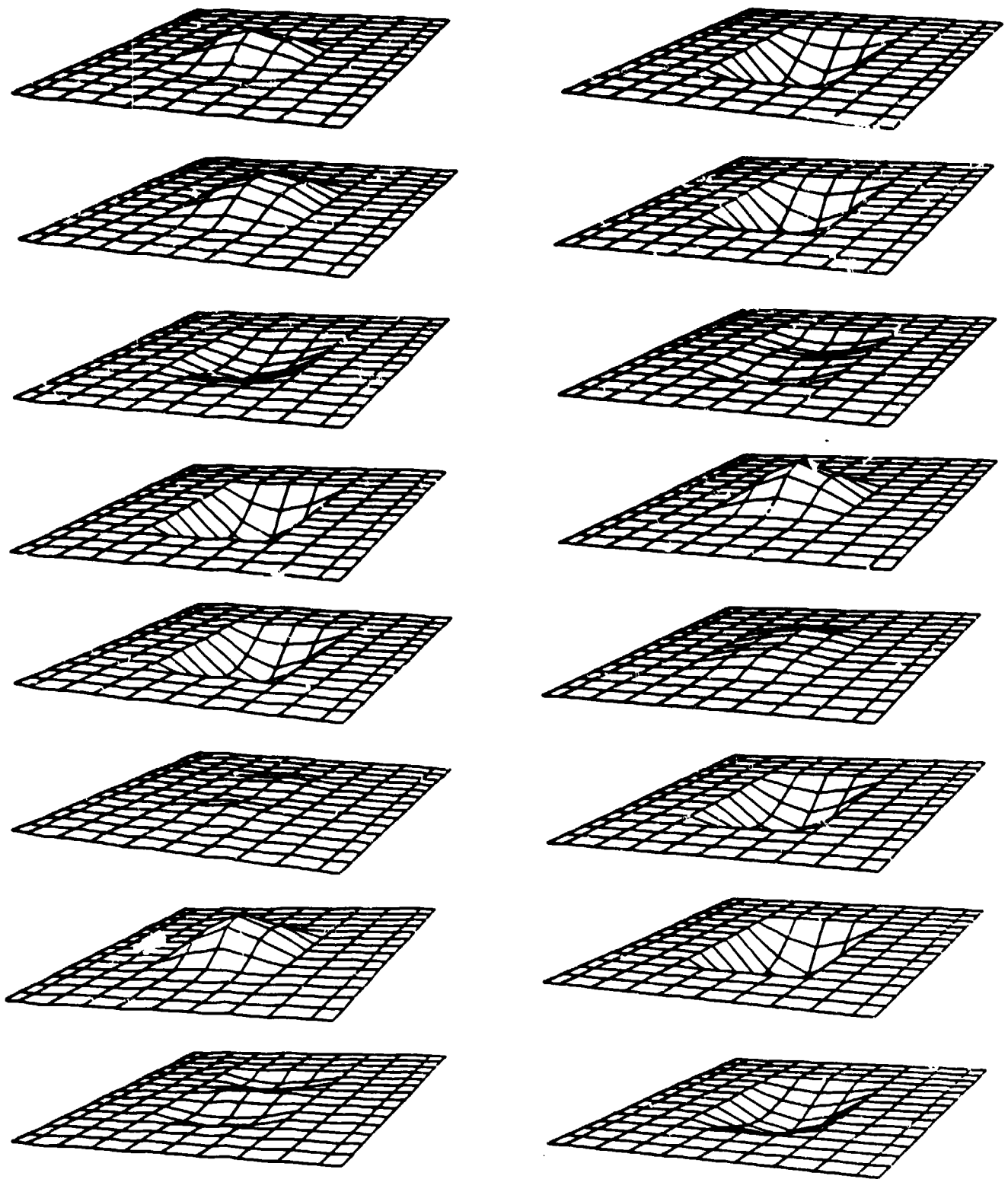


Figure 2-3. (Cont'd).

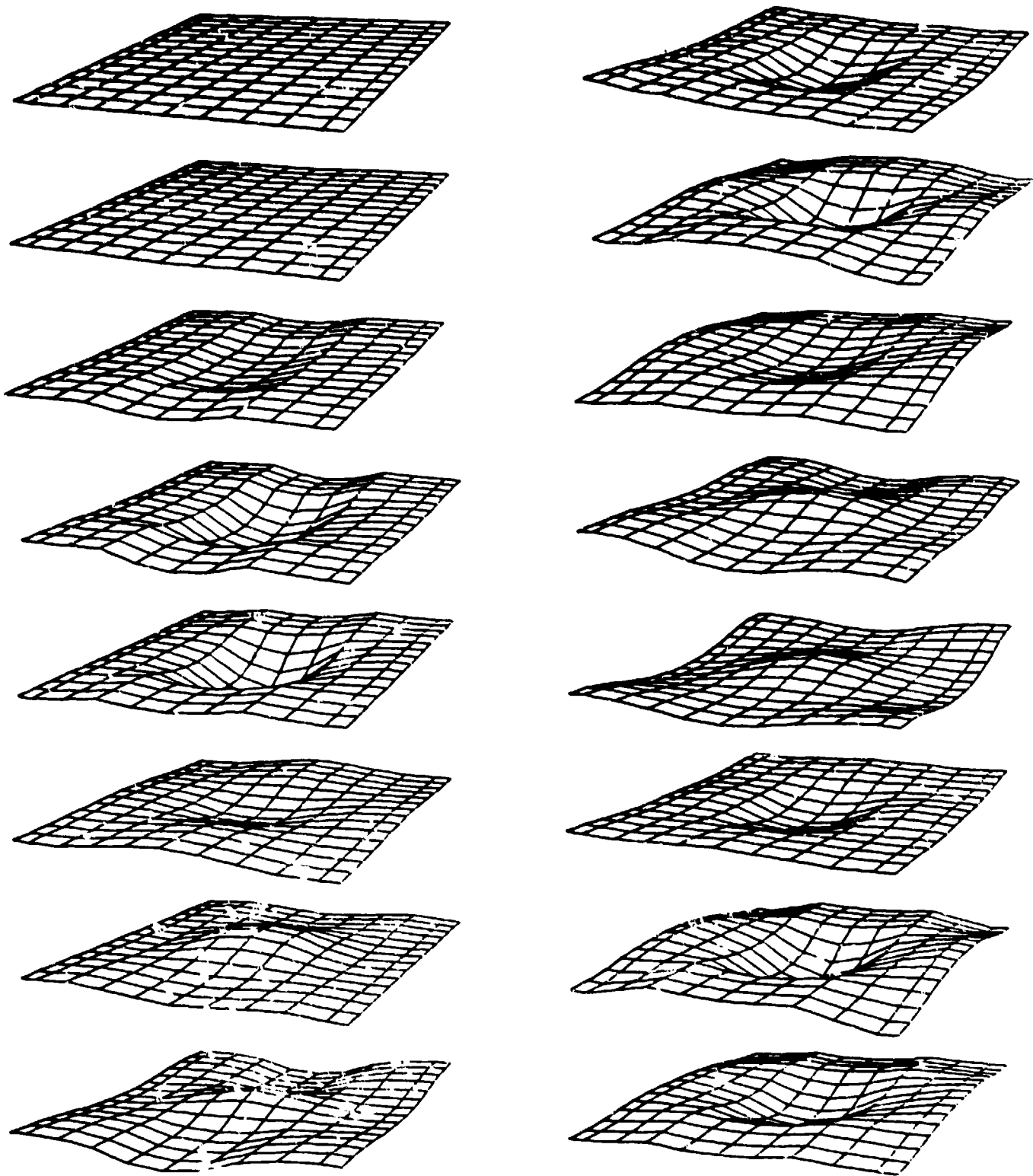


Figure 2-4. Displacement time history for top surface when tube is filled with water and bubble is at the center of the tube. Young's modulus for the skin is 1500 psi.

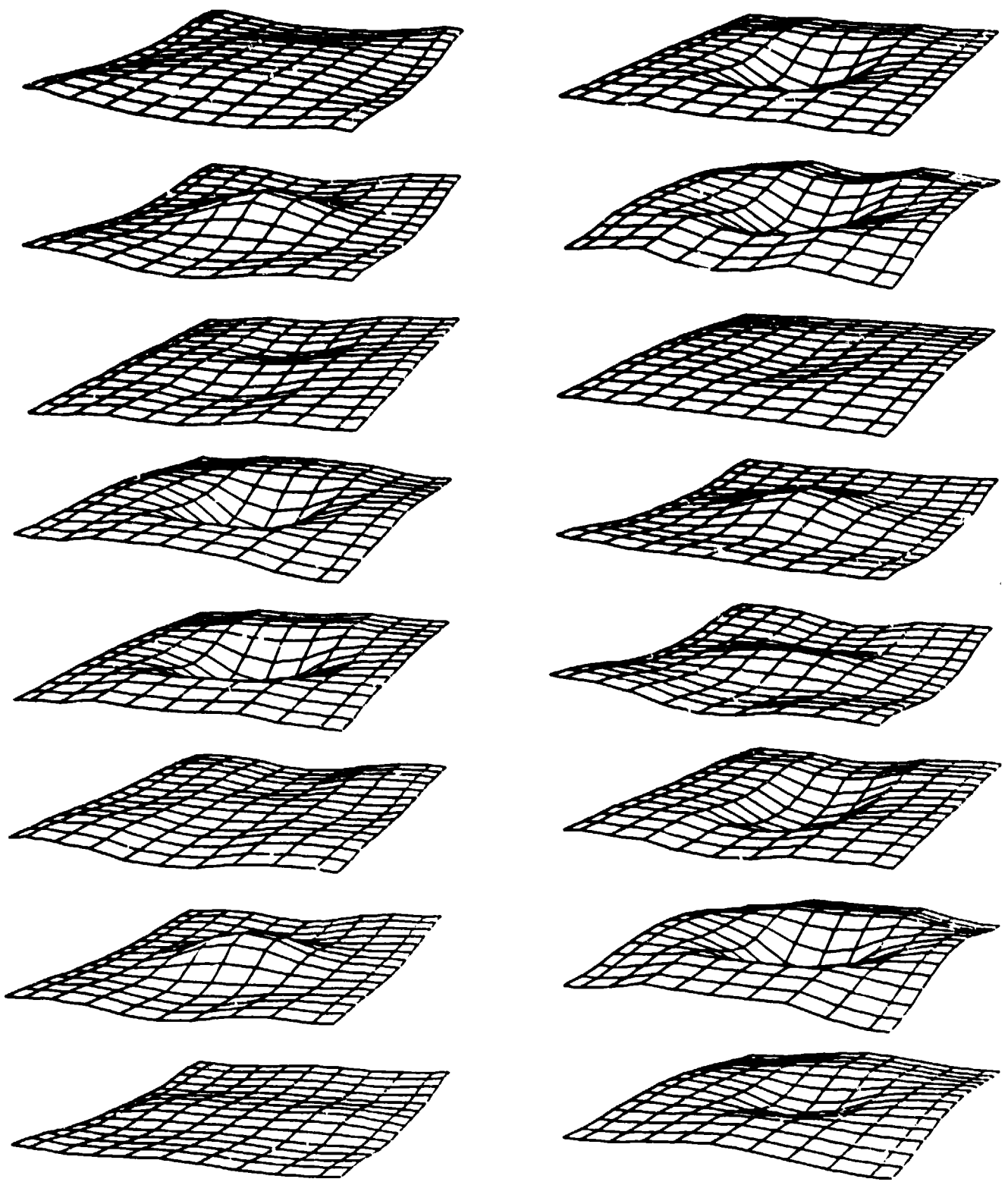


Figure 2-4. (Cont'd).

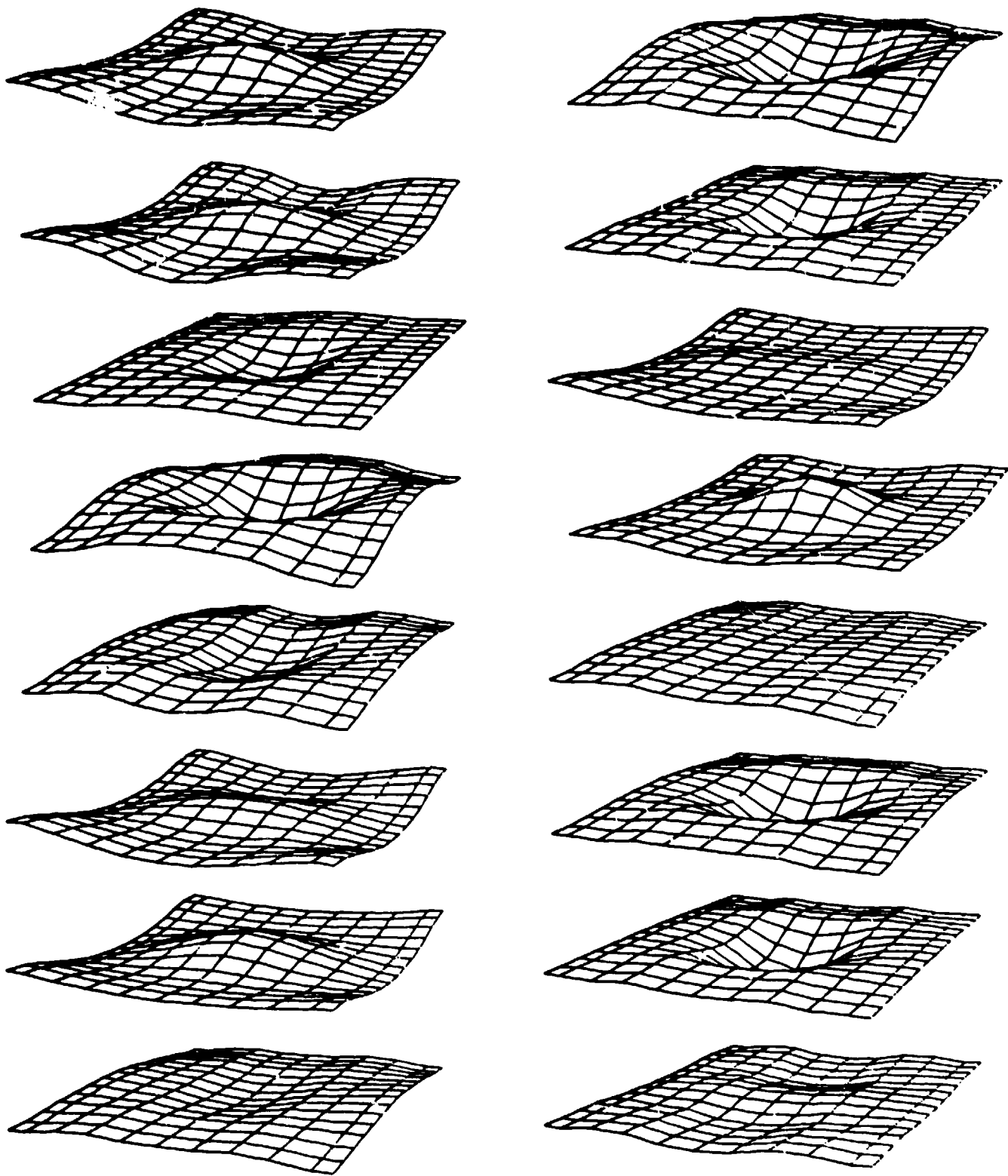


Figure 2-4. (Cont'd).

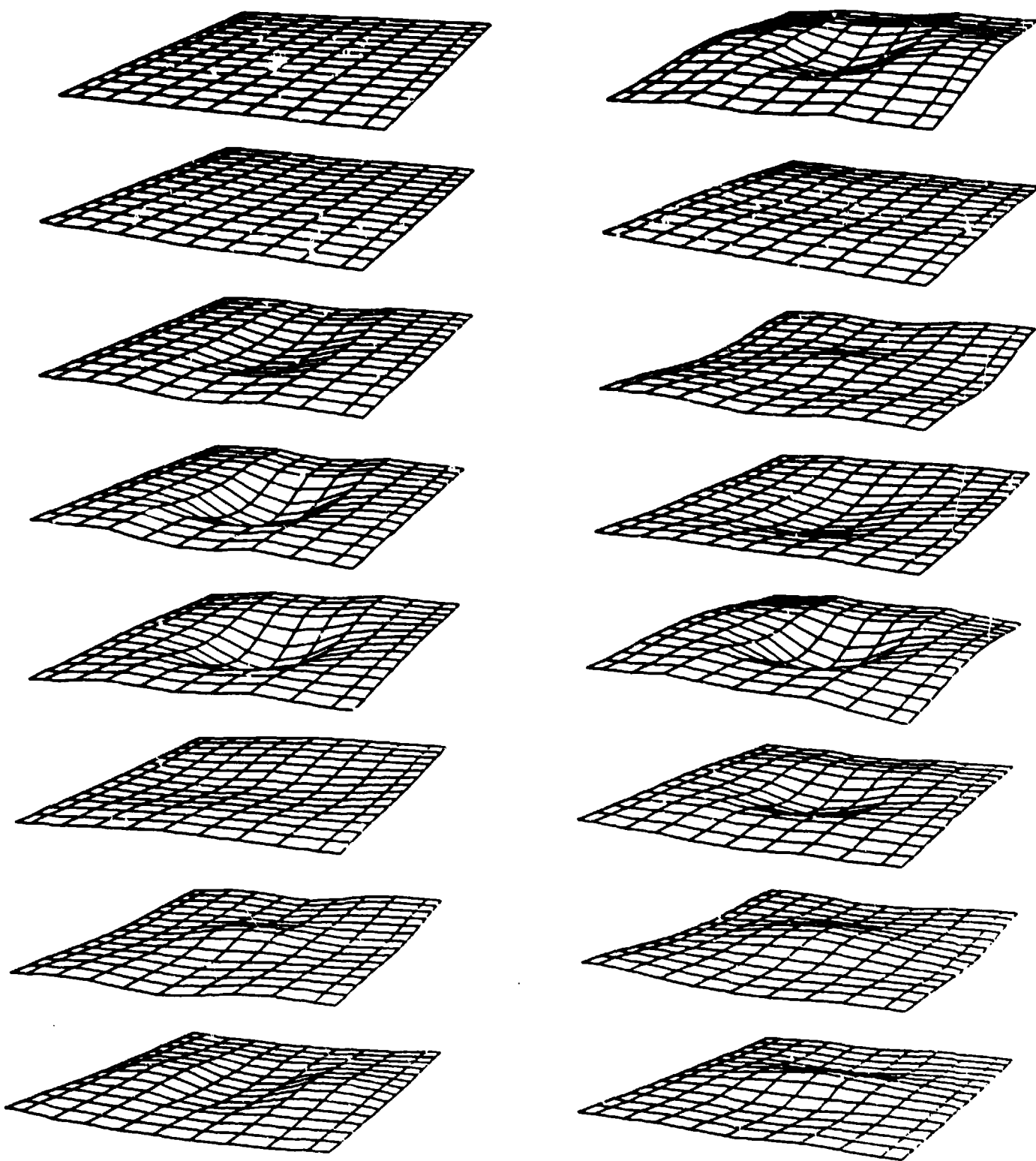


Figure 2-5. Displacement time history for top surface when tube is filled with water and bubble is at the center. Young's modulus for the skin is 3000 psi.

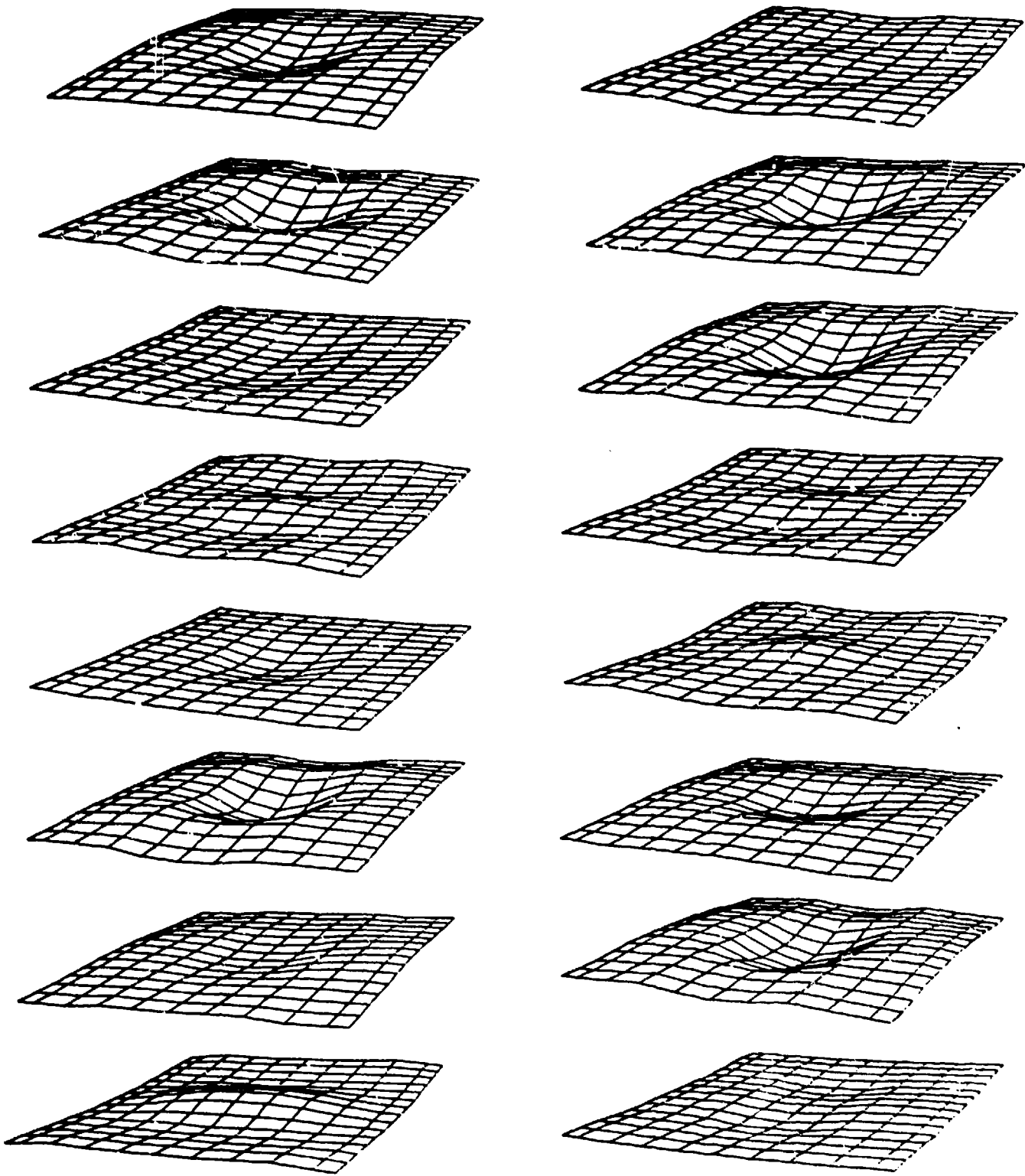


Figure 2-5. (Cont'd).

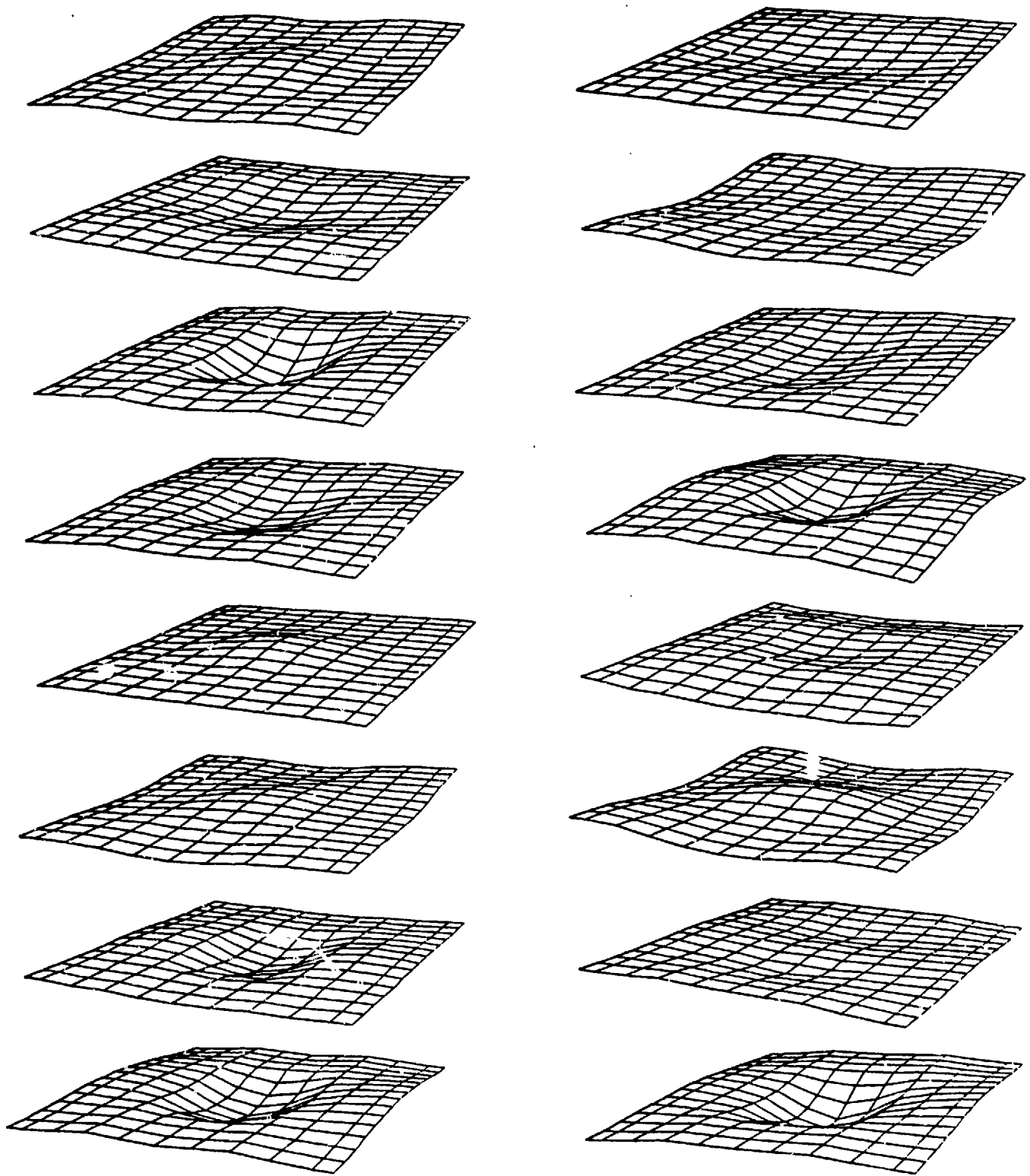


Figure 2-5. (Cont'd).

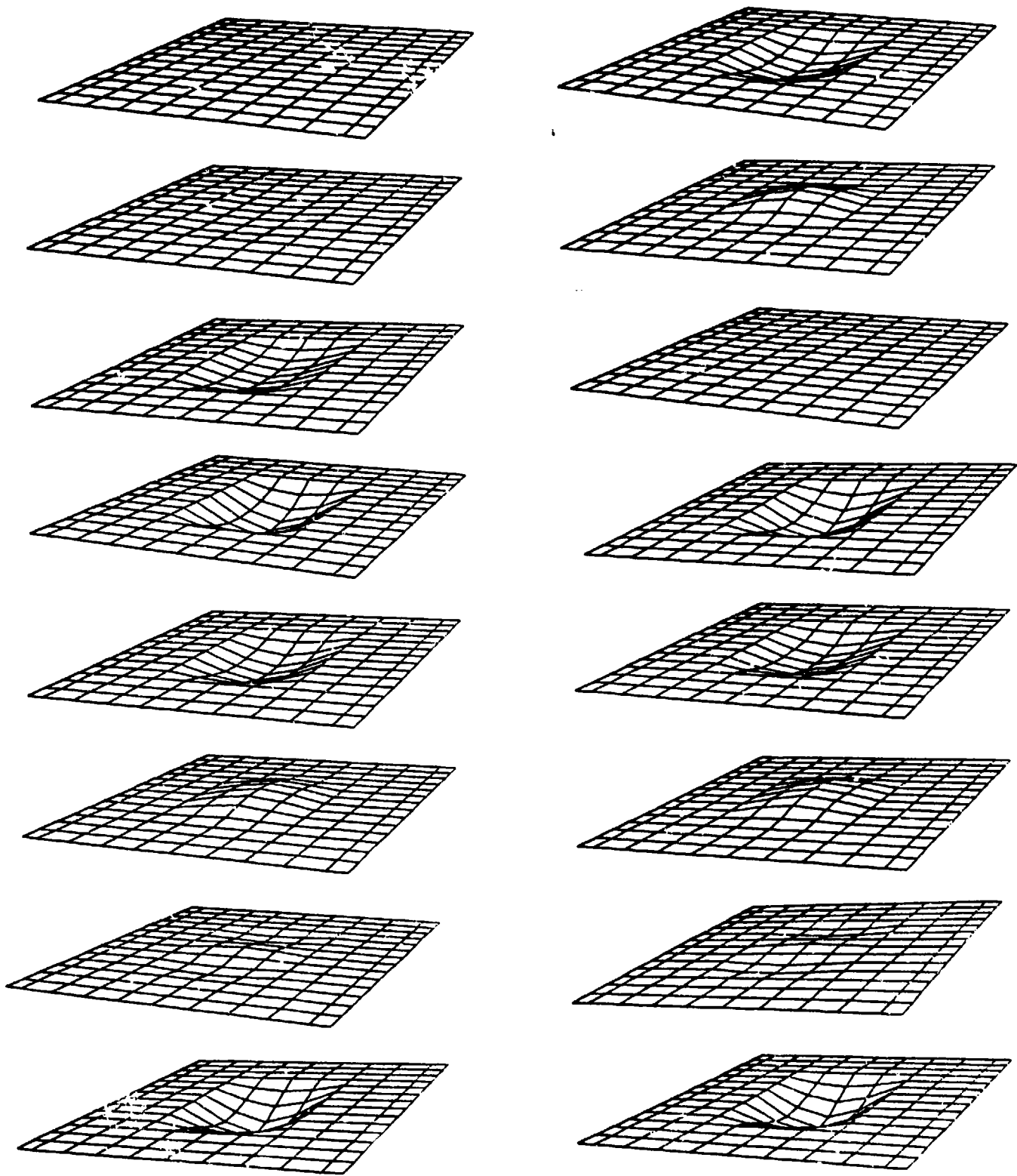


Figure 2-6. Displacement time history for top surface when tube is filled with water and bubble is at top. Young's modulus for skin is 3000 psi.

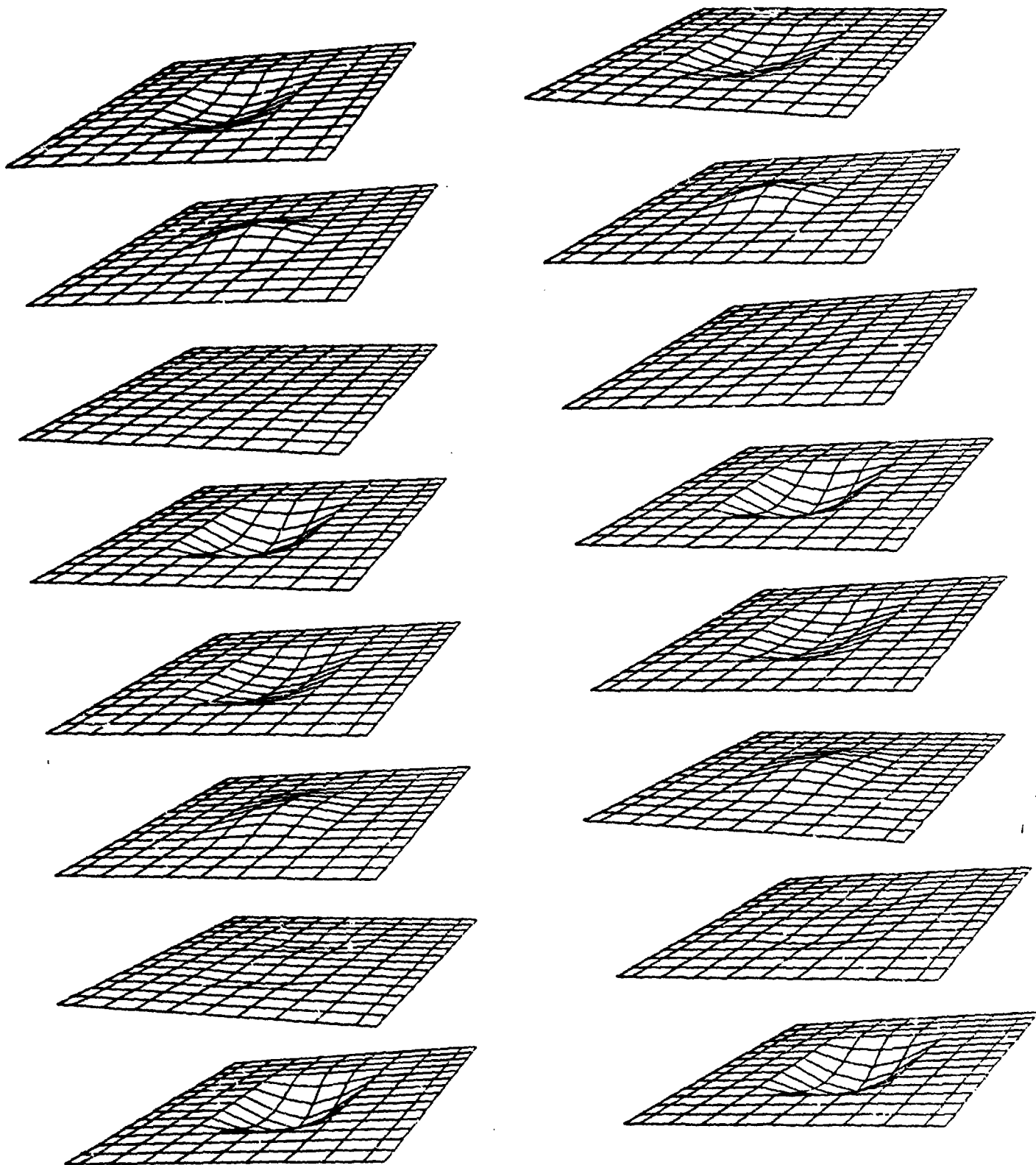


Figure 2-6. (Cont'd).

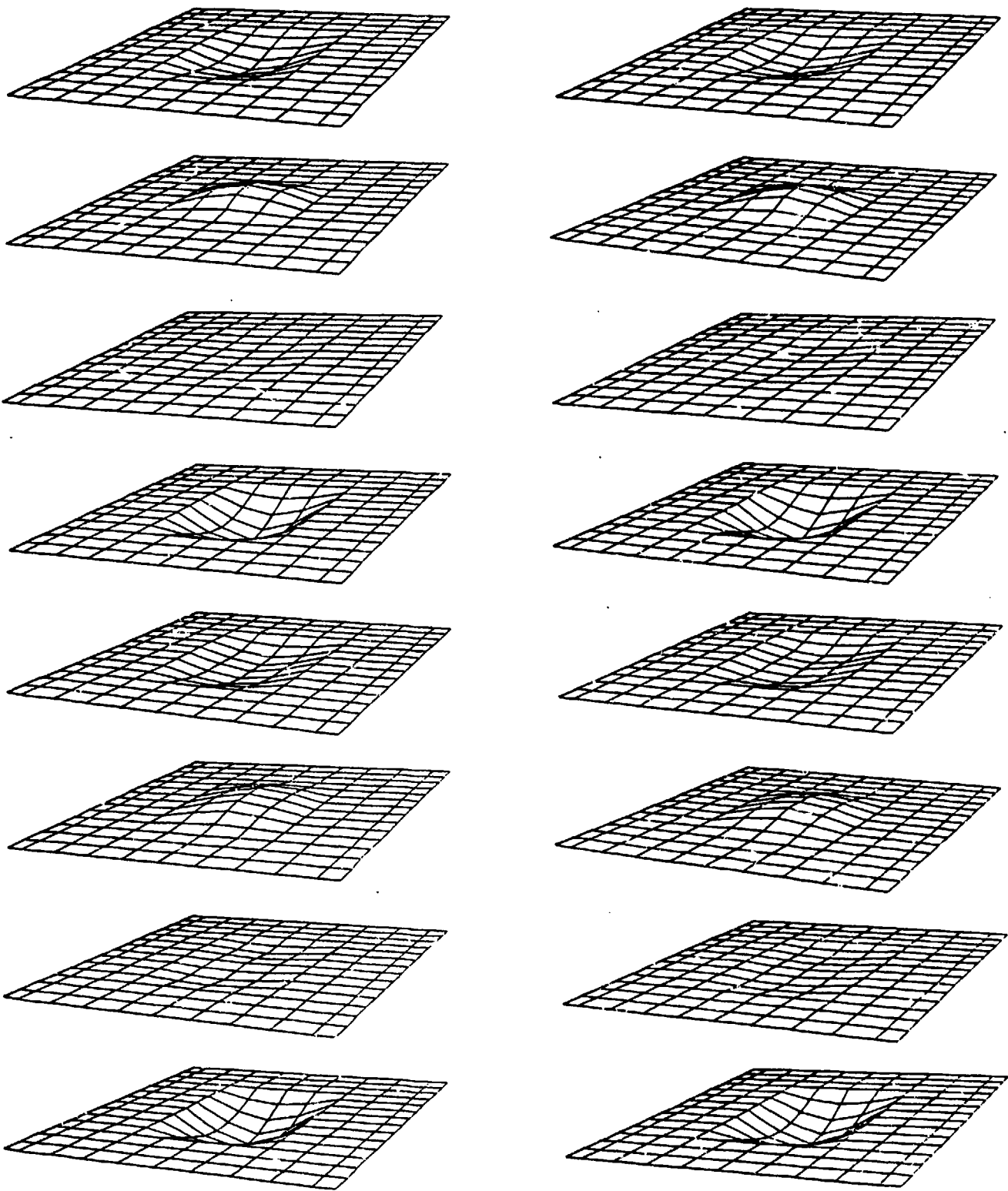


Figure 2-6. (Cont'd).

3. LABORATORY TESTS OF BLAST EFFECTS ON SIMULATED GASTROINTESTINAL EMBOLI

Evidence collected in the field has shown that blast overpressure (BOP) can cause localized gastrointestinal tract bleeding. This was suspected to be the result of localized intestinal lining strain associated with wall deformation caused by the collapse of entrapped gas bubbles near the membrane wall. Direct detection of the causal relationship will involve sophisticated equipment and instrumentation. However, a simple laboratory experiment provides some insight into the underlying mechanism. With this objective in mind, a series of simple experiments were conducted using the jet impactor and existing JAYCOR equipment.

The experiments were done by suspending a model "intestine" in a water chamber and then impacting the chamber's flexible "abdomen" to generate an equivalent BOP. Subsequent intestinal surface deformation was then recorded by a high speed movie camera for later analysis.

In these tests a number of air bubble sizes, impulse pressure magnitudes, and intestinal fluids were used. A brief description of the experimental setup and the findings are given below.

EXPERIMENTAL SETUP

Figures 3-1 and 3-2 show the arrangement of the single valve impactor used to fire a vertical blast at the representative GI tract model. Vertical firing was chosen to allow the camera to look down directly at the position where the air bubble contacted the simulated "intestine" wall. Figure 3-3 shows the nozzle head and orifice plate assembly. The orifice plate has a symmetrical non-expanding hole pattern, and the valve is an Asco 1.5" D.C. valve.

The "GI tract" pressure chamber model is shown in Figure 3-4. It is an aluminum cylinder filled with water, capped on one end by a 3/8" thick plexiglass window for viewing the subject, and capped on the bottom end by a 1/16" flexible rubber membrane simulating the abdomen's outer wall.

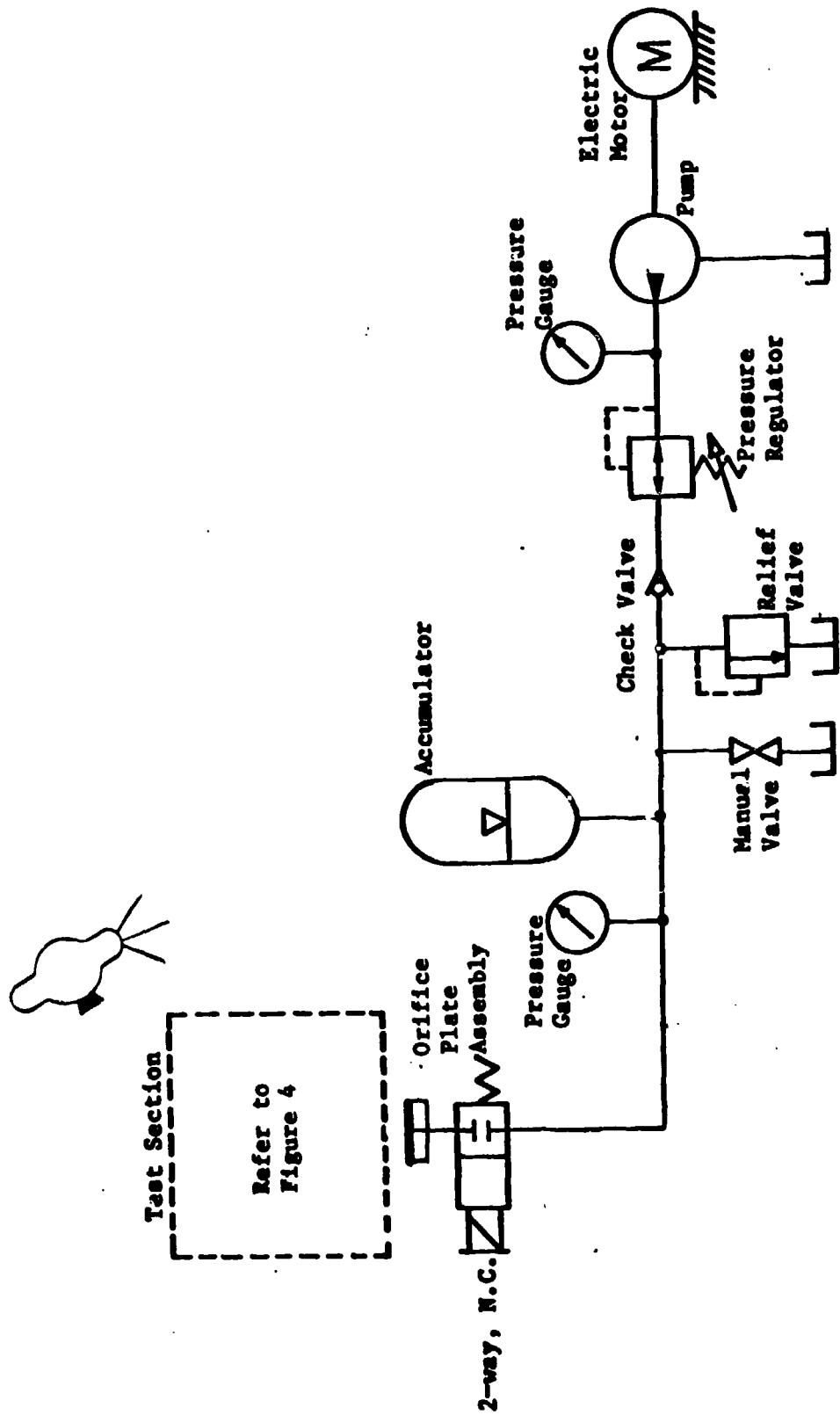


Figure 3-1. Schematic of jet impactor test setup.

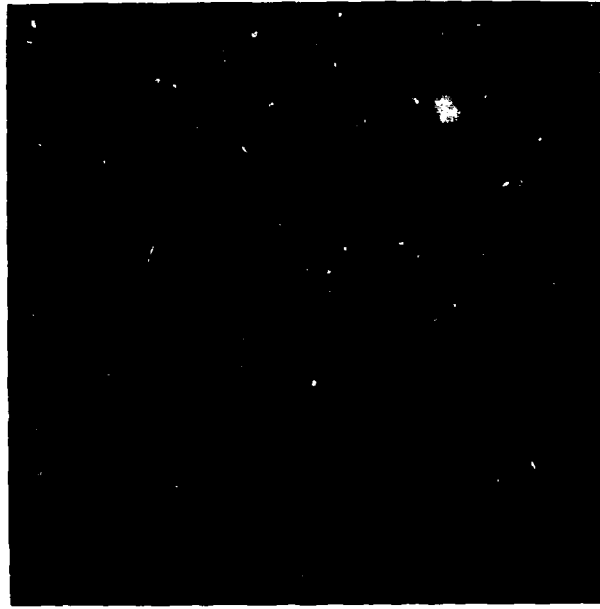


Figure 3-2. Experimental setup.



Figure 3-3. Valve and orifice plate assembly.

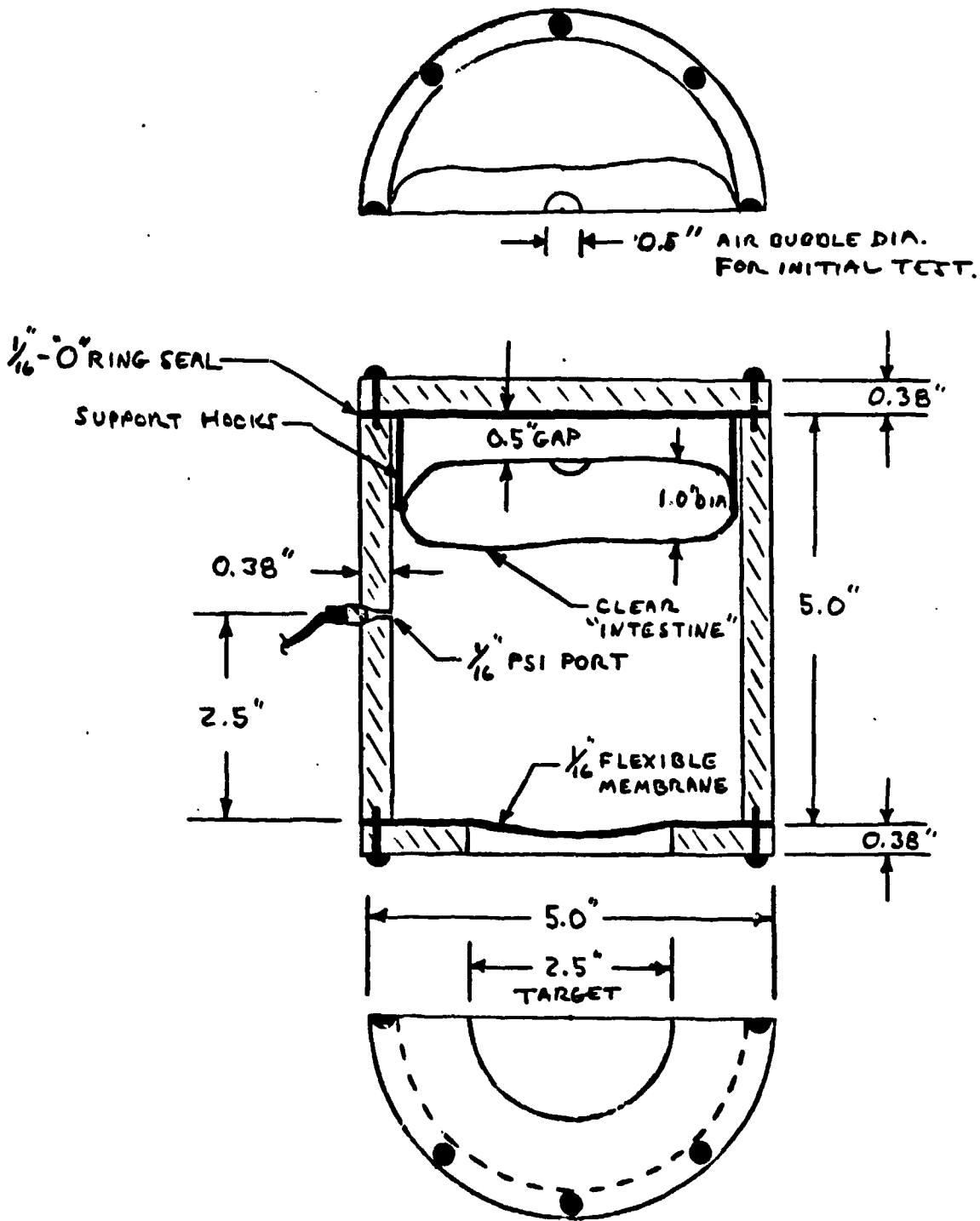


Figure 3-4. Cut-away view of pressure chamber setup for simulated GI tract bubble experiment.

Figure 3-5 shows the water filled GI tract model with a 0.5" air bubble (embolus). The GI model is a 1 mil thick closed tube made from plastic film and filled with water. The sealed "intestine" was suspended 0.5" from the viewing port. The entire chamber was filled with water and bled of any stray air bubbles. A pressure transducer with 1/16" diameter pressure port was installed (Fig. 3-6) in the chamber wall.

The GI tract model assembly was suspended at a target stand-off distance of 16 inches. The accumulator was charged to 140 psi and the impactor's system pressure was set at 180 psi. The valve cycle time was 120 ms.

A Fastax high speed movie camera was used to visualize the phenomenon of air bubble collapse and the associated membrane wall deformation. The photographic results were collected onto a single reel and delivered separately to WRAIR.

TEST RESULTS AND DISCUSSION

A typical pressure signal measured at the cylinder wall is shown in Figures 3-7 and 3-8. A relatively high initial impact pressure of 48 psi was used for the initial test to insure an observable impact effect on the air bubble. The results can be seen in movie "C." A second movie, "N," was made using an 1.0" air bubble in water. This larger bubble showed similar reactions to the blast. The test matrix and test parameters for these and subsequent tests are summarized in Table 3-1.

The initial tests confirmed that the high speed camera could "see" the blast-induced contraction of the air bubble. Closer examination indicated correlation of air bubble collapse and expansion with pressure signal shape. Figure 3-9 qualitatively correlates bubble motion with the measured pressure. The effects of the bubble collapse on the membrane wall dynamics became the next visualization objective.

To enhance the quality of the test results, a higher speed (ASA 400) color movie film was used for the remaining tests, and the Fastax exposure rate was increased from 2400 to 4000 frames per second.



Figure 3-5. Initial test installation with 0.5" air bubble.

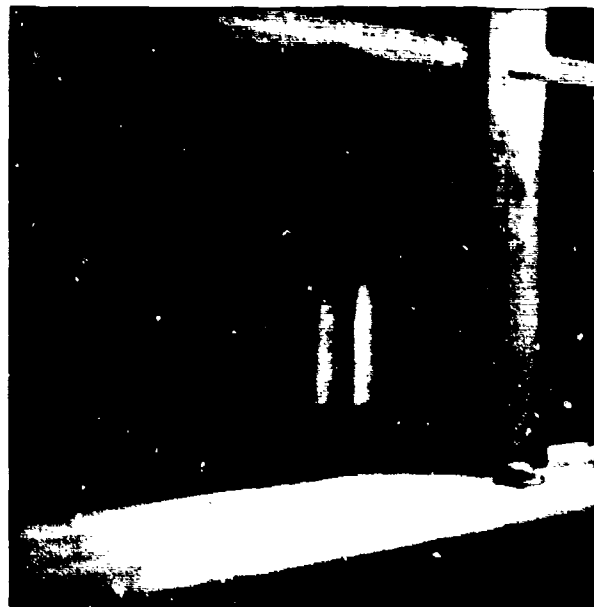


Figure 3-6. Transducer location on test chamber wall.

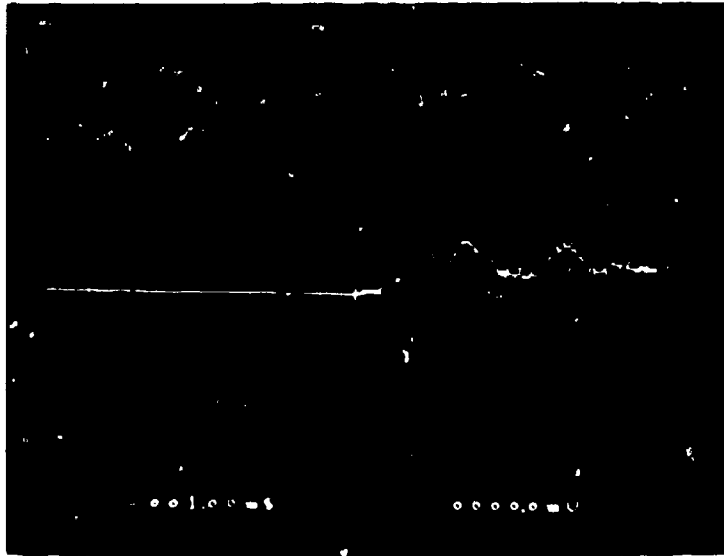


Figure 3-7. Initial peak.

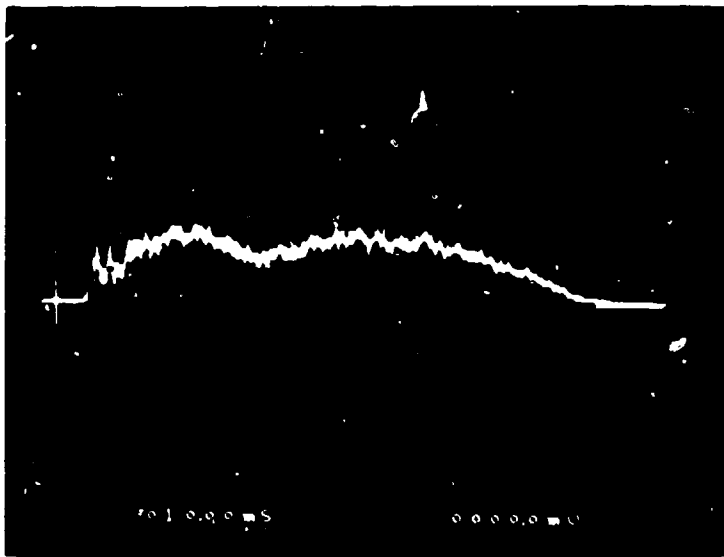


Figure 3-8. Typical full impulse shape.

Table 3-1. Test Matrix

Movie	Date	Bubble Size (in.)	Rise Time (ms)	Max. Press. (psi)	Initial Impulse (ms)	Hump (psi)	Total Signal (ms)	Membrane Fluid
C	4/27	0.5	0.75	48	4.5	13	118	water
N	6/21	1.0	1.15	30	4.9	10	153	water
I	6/18	2.0	1.55	36	3.2	13	154	milk of magnesia
J	6/18	2.0	1.45	26	3.2	16	> 184	milk of magnesia
L	6/21	2.0	2.50	8	5.2	7	112	milk of magnesia
K	6/18	2.0	2.76	2	6.3	-	8	milk of magnesia
M	6/21	0.5	0.75	39	3.9	7	163	milk of magnesia
H	6/18	-	1.30	51	4.0	13	> 190	milk of magnesia
P	6/25	1.0	1.25	47	2.6	15	168	gel paste

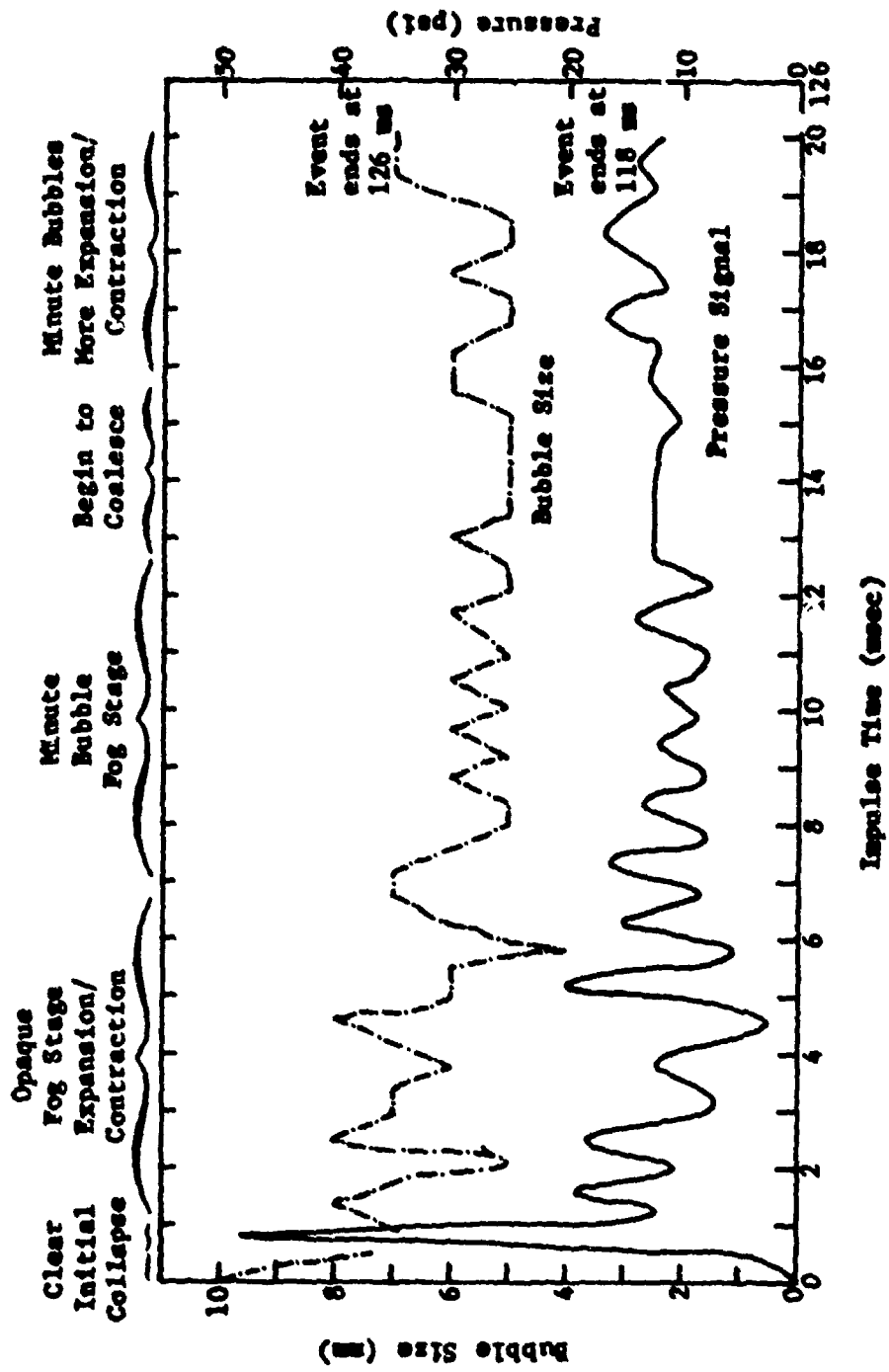


Figure 3-9. Correlation of bubble motion with pressure.

Movies H through M used the GI model shown in Figures 3-10 and 3-11. The intestine model was again made of 1 mil thick plastic film, however this time it was filled with milk of magnesia to give an opaque background so that the grid lines drawn on the "skin" of the model to show surface distortion could easily be seen.

Movie "I" shows the results of a test with a 2.0" air bubble submitted to a shock wave of 36 psi with a rise time of 1.55 ms. The film shows a dramatic cratering of the membrane wall around the bubble as the impulse strikes the model. The continued pressure by the "hump" section of the signal prevents the crater from restoring immediately to its original equilibrium position until the entire impulse signal had passed.

Movie "J" shows the same test setup at 26 psi with a rise time of 1.45 ms. The results are similar to Movie "I".

Movie "L" shows the effects of an 8 psi shock wave with a rise time of 2.50 ms. Even at this relatively low pressure, deformation of the membrane wall can still be seen.

Movie "K" shows that at 2 psi and a rise time of 2.76 ms no discernible wall deformation effect can be seen for this particular membrane material.

Movie "M" shows the effects on a 0.5" air bubble. Under a pressure of 39 psi and a rise time of 0.75 ms. The smaller air bubble shows a much more localized reaction than with the 2.0" air bubble.

Movie "H" is a null test. No bubble was present in the model. A shock wave of 50 psi with a rise time of 1.30 ms was applied. The results show no visible effect on the membrane wall.

Movie "P" shows the effects of a 47 psi shock wave with a rise time of 1.25 ms on a 1.0" bubble entrained in a denser gel made of toothpaste. The results show similar membrane wall reaction but the thicker fluid appears to dampen the propagation of surface distortion.

These results show that the bubble volume changes in correlation with impulse pressure. Furthermore, the bubble volume change causes the membrane wall to crater and fill the "void" left by the collapsed air bubble.



Figure 3-10. Intestine model.

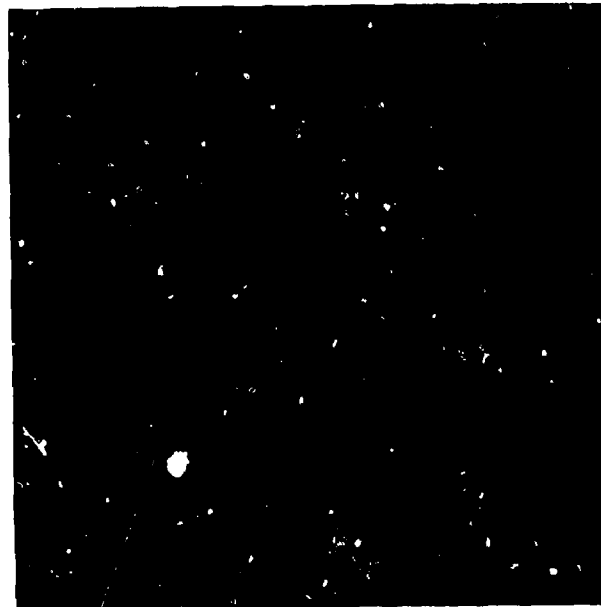


Figure 3-11. Intestine model installation.

Though the model used in this experiment differed in material properties from that of a real intestine, it is plausible that the observed cratering effect and subsequent bulging of the membrane wall could be related to the cause of the localized gastrointestinal wall trauma seen in the animals.

DISTRIBUTION LIST

12 copies Director
Walter Reed Army Institute of Research
Walter Reed Army Medical Center
ATTN: SGRD-UWZ-C
Washington, DC 20307-5100

1 copy Commander
US Army Medical Research and Development Command
ATTN: SGRD-RMI-S
Fort Detrick, Frederick, Maryland 21701-5012

12 copies Defense Technical Information Center (DTIC)
ATTN: DTIC-DDAC
Cameron Station
Alexandria, VA 22304-6145

1 copy Dean
School of Medicine
Uniformed Services University of the
Health Sciences
4301 Jones Bridge Road
Bethesda, MD 20814-4799

1 copy Commandant
Academy of Health Sciences, US Army
ATTN: AHS-CDM
Fort Sam Houston, TX 78234-6100